Le 2ème Séminaire International sur les Energies Nouvelles et Renouvelables
The 2nd International Seminar on New and Renewable Energies
Unité de Recherche Appliquée en Energies Renouvelables,
Ghardaïa – Algérie 15, 16 et 17 Octobre 2012

Numerical Investigation of Latent Thermal Energy Storage in Shell-and-Tube Configuration

Mohammed Bechiri, Kacem Mansouri

Energy and Mechanical Engineering Laboratory, University M. Bougara, Boumerdès, 35000, Algeria

bechiri_med@yahoo.fr

manskac@yahoo.fr

***Abstract*— A thermal energy storage system in a tube of Phase Change Material (PCM), with laminar fluid flow inside a duct, was numerically studied. The melting and solidification of the PCM was solved numerically by using the enthalpy method with adopting the finite difference scheme for both PCM and heat transfer fluid (HTF). The axial heat conduction in the PCM wall and the HTF is considered. The effects of various parameters on the storage system was studied and treated; The charging/discharging process is investigated in terms of liquid–solid interface position, liquid fraction, total heat transmitted to PCM and thermal storage efficiency for various HTF working conditions.**

***Keywords*— latent heat storage, enthalpy method, shell-and tube configuration.**

I. Introduction

Due to the advantage of the large heat storage capacity and isothermal behaviour during the charging and discharging processes, latent thermal energy storage (LTES) systems have been widely used in solar energy system, industrial waste heat recovery and electrical power load shifting application in recent years. There are many storage techniques available including the phase change materials (PCM) used in packed bed latent thermal energy storage systems [1-10]. In ref. [[1]], the transient heat transfer phenomenon during technical grade paraffin melting and solidification, in the shell-and-tube latent thermal energy storage system with water as heat transfer fluid (HTF) has been analyzed both numerically and experimentally. Lacroix [[2]] studied numerically and experimentally the behavior of a latent heat transfer energy storage unit with a finned tube. Ismail and Goncalves [[3]] analyzed numerically the thermal performance of a PCM storage unit with a constant heat transfer coefficient between working fluid and the tube wall.

Cao and Faghri [[4]] simulated numerically the turbulent conjugated forced convection of the shell-and-tube thermal energy storage system with a working fluid at low Prandtl number. Ismail and Abugderah [[5]] studied a vertical tube performance of a phase change thermal energy storage system. The momentum and the energy equations are solved numerically. Studies on using PCMs with solar devices were carried out experimentally by Mawire and McPherson [[6]] who charged thermal energy storage of a solar cooker at constant temperature and variable electrical power. Chen et al. Reddy [[7]] used thermal modeling and analysis of a transparent insulation materials covered solar integrated collector storage water heating system with PCM. Bellecci and Conti [[8]], using the enthalpy method, studied numerically the cyclic behaviour of a phase change solar shell and tube energy storage module. Ait Adine and Qarnia [[9]] studied numerically a latent heat storage unit consisting of a shell and tube filled with two phase change materials, P116 and n-octadecane. Tao and He [[10]] performed the numerical study on the TES performance. The effects of the unsteady inlet temperature and mass flow rate are examined.

The first objective of the present work is to elaborate a numerical solution to predict the thermal behavior of the latent energy storage system (LESS), consisting of several tubes of phase change material (PCM). The working fluid (water) circulating on laminar regime within the ducts charges and discharges the storage unit. The second objective is to develop a parametric study to evaluate the effect of the HTF inlet temperature on the performance of the storage unit.

II. Mathematical Modelling and Resolution

The latent thermal energy storage system analyzed in this paper is shown in Fig. 1.

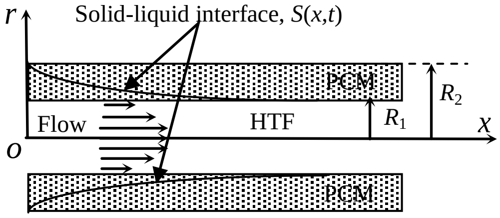

Fig. 1 Geometry of considered duct.

It is consists of one tube with adiabatic outer radius boundary condition and constant inlet temperature, in which the working fluid flows by laminar forced convection. With the enthalpy method, the governing energy equation is written for the entire region of the PCM, including solid and liquid phases and the interface.

HTF region

$$\frac{\partial T_f(x,r,t)}{\partial t}+u(r)\frac{\partial T_f(x,r,t)}{\partial x}=\frac{\alpha_f}{r}\frac{\partial}{\partial r}\left(r\frac{\partial T_f(x,r,t)}{\partial r^2}\right) \quad x,t>0 \quad (1)$$

$$T_f(0,r,t)=T_0, \qquad t>0, \qquad (2)$$

$$\left.\frac{\partial T_f(x,r,t)}{\partial x}\right|_{x=L}=\left.\frac{\partial T_f(x,r,t)}{\partial r}\right|_{r=0}=0, \qquad x,t>0, \qquad (3)$$

$$T_f(x,y,t)=T_{\text{int}}, \qquad t=0 \qquad (4)$$

PCM region

$$\frac{k_{pcm}}{r}\frac{\partial}{\partial r}\left(r\frac{\partial T_{pcm}(x,r,t)}{\partial r^2}\right)=\rho_{pcm}\frac{\partial H(x,r,t)}{\partial t}, \qquad x,t>0, \quad (5)$$

$$\left.\frac{\partial T_{pcm}(x,r,t)}{\partial r}\right|_{r=R_2}=0, \qquad r=R_2,\ x>0,\ t>0, \qquad (6)$$

$$\left.\frac{\partial T_{pcm}(x,r,t)}{\partial x}\right|_{x=0}=\left.\frac{\partial T_{pcm}(x,r,t)}{\partial x}\right|_{x=L}=0, \qquad t>0, \qquad (7)$$

$$T_{pcm}(x,y,0)=T_{\text{int}} \qquad x>0,\ t=0. \qquad (8)$$

Interface PCM-HTF

$$k_f\frac{\partial T_f(x,r,t)}{\partial r}=k_{pcm}\frac{\partial T_{pcm}(x,r,t)}{\partial r},$$

$$r=R_1,\ x>0,\ t>0, \qquad (9)$$

$$T_f(x,r,t)=T_{pcm}(x,r,t), \qquad r=R_1,\ x>0,\ t>0, \qquad (10)$$

The enthalpy, H, is a function of temperature, T:

$$H(T)=\begin{cases} cp_{pcm}(T-T_m) & T<T_m \\ cp_{pcm}(T-T_m)+q & T>T_m \end{cases} \qquad (11)$$

and at the melting point of the PCM, the enthalpies of solid and liquid phases at the melting point are 0 and q, respectively.

In the following, we will adopt the numeric resolution with using the Finite Difference Method, each location and time are represented by i, j and n.

$$T_{i.j}^{n}=T(x,r,t)=T(j.\Delta x,i.\Delta r,n\Delta t)$$

Equations system (1-10) is discretized by using an explicit scheme which uses forward difference in time and central difference in space. Then, the temperature distribution is obtained as:

HTF region

$$T_{f\ i.j}^{\ n+1}=\left(1-2\frac{\Delta t\ \alpha_f}{\Delta r^2}\right)T_{f\ i.j}^{\ n}-\frac{\Delta t\ u_b}{\Delta x}\left(1-\left(\frac{i\ \Delta r}{R_1}\right)^2\right)\left(T_{f\ i.j+1}^{\ n}-\right.$$

$$\left.T_{f\ i.j-1}^{\ n}\right)+\frac{\Delta t\ \alpha_f}{\Delta r^2}\left(T_{f\ i+1.j}^{\ n}+T_{f\ i-1.j}^{\ n}+\frac{T_{f\ i+1.j}^{\ n}-T_{f\ i-1.j}^{\ n}}{2\ i}\right),$$

PCM region

$$H_{i.j}^{n+1}=H_{i.j}^{n}+\frac{\Delta t\ k_{pcm}}{\rho_{pcm}(\Delta r)^2}\left(T_{pcm\ i+1.j}^{\ n}-2\ T_{pcm\ i.j}^{\ n}+T_{pcm\ i-1.j}^{\ n}\right.$$

$$\left.+\frac{T_{f\ i+1.j}^{\ n}-T_{f\ i-1.j}^{\ n}}{2\ i}\right)$$

PCM-HTF interface

$$T_{i.j}^{n+1}=\frac{k_{pcm}\ T_{pcm\ i+1.j}^{\ n}+k_f\ T_{f\ i-1.j}^{\ n}}{k_{pcm}+k_f}$$

after the PCM enthalpy distribution of the $(n+1)^{th}$ time step is obtained, the temperature distribution of the $(n+1)^{th}$ time zone can be obtained from equation (11) as:

$$T_{pcm\ i,j}^{\ n+1}=\begin{cases} T_m+H_{i,j}^{n+1}/cp_{pcm} & H_{i,j}^{n+1}\le 0 \\ T_m & 0<H_{i,j}^{n+1}<q \\ T_m+\left(H_{i,j}^{n+1}-q\right)/cp_{pcm} & H_{i,j}^{n+1}\ge q \end{cases}$$

If the enthalpy at a certain point $P_{i,j}^{n+1}$ satisfies 0 <H< q, the solid-liquid interface coordinate will be:

$$S(x,t)=S_j^{n+1}=\left(i.\Delta r,(n+1).\Delta t\right).$$

Thermal energy storage efficiency, δ, defined as the ratio between the energy stored to the maximum energy stored, and it is expressed as:

$$\delta = \frac{fr\, q\, L\, \left(R_2^2 - R_1^2\right) + 2\, cp_{pcm} \int_{R_1}^{R_2} \int_0^L \left(T_{pcm} - T_{\text{int}}\right) r\, dx\, dr}{L\, \left(R_2^2 - R_1^2\right)\left(q + cp_{pcm}\left(T_0 - T_{\text{int}}\right)\right)},$$

where the liquid fraction *fr* can be calculated by

$$fr = \frac{\int_0^L \left(S^2 - R_1^2\right)\, dx}{L\, \left(R_2^2 - R_1^2\right)}.$$

III. Results and Comments

In the present study, water is used as the HTF material, and Paraffin is used as a latent heat energy storage material, the melting point temperature and the density are important parameters, whose values are shown in table 1.

TABLE I
THEM-PHYSICAL PROPRIETIES OF THE PARAFFIN AND WATER

	Paraffin	water
Melting/solidification temperature (*K*)	300.7	/
latent heat capacity ($kJ\ kg^{-1}$)	206	/
Thermal conductivity ($W\ m^{-1}\ K^{-1}$)	0.18	0.6
Specific heat ($kJ\ kg^{-1}\ K^{-1}$)	1.8	4182
Density ($kg^{-1} m^{-3}$)	789	998.2
Viscosity ($m^2\ s^{-1}$)	/	1.005E-6

A series of numerical calculations have been done during the melting of the technical grade paraffin at fixed HTF working condition (Re = 1200). The initial temperature distribution in both HTF and PCM regions is T_i=280 K.

Fig. 2, displays the transient temperature profiles during melting at some typical transversal points at x=1.5 m, in the first stage the material stores energy primarily by sensible heat at all locations during about 20 min. During the second stage, the energy is charged by latent heat, the phase change progress until the melting process in all thickness of PCM is completed, at the end of melting process, a more rapid increase of PCM temperature was observed. The third stage starts when all the PCM is melted. During this stage, energy is charged by sensible heat under a fusion form until reaching the steady state.

Fig. 3 shows the instantaneous solid–liquid interface distribution along the duct. Note that for a duct length ($x \leq$ 0.4m), all the PCM is melted at time t = 50min. However, the PCM so far from the duct inlet is remained at a solid phase.

Fig. 4 displays the time wise variations of the liquid fraction, *fr*, and the thermal storage efficiency, δ, for different HTF inlet temperature. As the time progress, the storage efficiency, δ, increases monotonically until a maximum value (equal to 1). When the melting process is completed, the liquid fractions *fr* is equal to 1. The corresponding thermal storage efficiency is lower than 1 (δ < 1). When the steady-state condition is reached, the PCM is completely melted and heated. The corresponding thermal storage efficiency is equal to 1. In other way, the storage time decreases with the increase of the HTF inlet temperature.

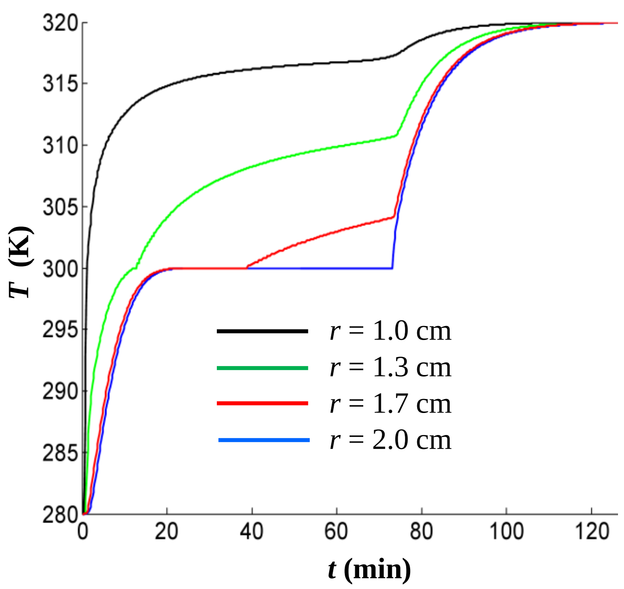

Fig. 2 Transient temperature profiles during melting at some typical transversal points at *x*=1.5m (r_1=1cm, r_2=2cm, Ste=0.175 and L=1.5m).

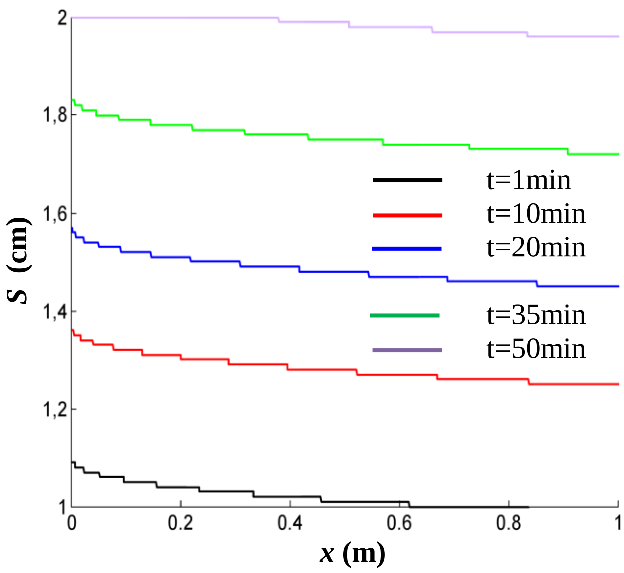

Fig. 3 Variation of liquid-solid interface along the duct for different time periods (r_1=1cm, r_2=2cm, Ste=0.175 and L=1m)

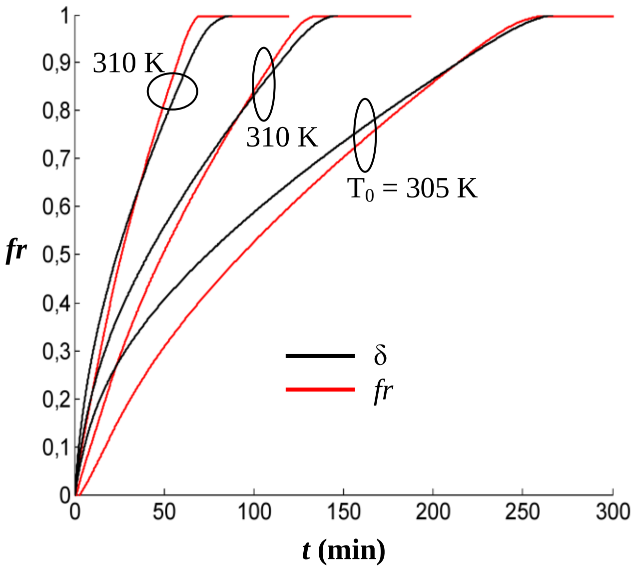

Fig. 4 Evolution of the liquid fraction and the thermal storage efficiency for different inlet temperature (r_1=1cm, r_2=2cm, Ste=0.175 and L=1m).

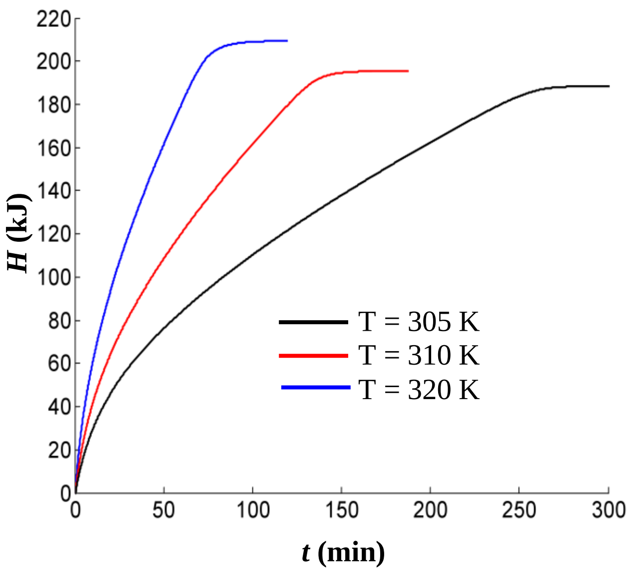

Fig. 5 Temporal variation of thermal energy stored for different inlet temperature (r_1=1cm, r_2=2cm, Ste=0.175 and L=1m).

The Fig. 5 shows the variation of the total energy stored in the PCM, for different HTF inlet temperature. It is clear that the amount of energy stored by sensible heat increases with increasing inlet temperature. On the other hand, the maximum time required for storage is reduced if the temperature of the fluid at the inlet is increased.

IV. Conclusions

In the present paper, the latent thermal energy storage system, which consists of shell-and-tube configuration, has been numerically studied by using enthalpy method. The working fluid circulating inside the channel is subjected to a constant inlet temperature. The thermal performance of energy storage unit is examined illustrating the specific influence of different parameters. The results obtained in the present study can be briefly summarized as follows:

1- The higher temperatures are fined near the HTF tube surface as a result of immediate melting of the PCM, and larger times are needed to reach the melting temperatures of the PCM.

2- The solid-liquid interface moves away more slowly from the HTF-PCM interface for high values of x, therefore the displacement of the solid-liquid interface is faster at the duct inlet.

3- The maximum time required for storage is reduced if the temperature of the fluid at the inlet is increased.

References

[1] A. Trp, “An Experimental and Numerical Investigation of Heat Transfer During Technical Grade Paraffin Melting and Solidification in a Shell-and-Tube Latent Thermal Energy Storage Unit”, *Solar Energy*, vol. 79, pp. 648–660, 2005.

[2] M. Lacroix, “Study of the Heat Transfer Behavior of a Latent Heat Thermal Energy Storage Unit with a Finned Tube”, *Int. J. Heat and Mass Transfer*, vol. 36, pp. 2083–2092, 1993.

[3] K. Ismail and M. Goncalves, “Thermal Performance of a PCM Storage Unit”, *Energy Conversion Management*, vol. 40, pp. 115–138, 1999.

[4] Y. Cao and A. Faghri, “A Study of Thermal Energy Storage Systems with Conjugate Turbulent Forced Convection”, *J. Heat Transfer*, vol. 114, pp. 1019–1027, 1992.

[5] K. Ismail and M. Abugderah, “Performance of a Thermal Storage System of the Vertical Tube Type”, *Energy Conversion Management*, vol. 41, pp. 1165–1190, 2000.

[6] A. Mawire and M. McPherson, “Experimental Characterization of a Thermal Energy Storage System Using Temperature and Power Controlled Charging”, *Renewable Energy*, 33, 669-682 (2008).

[7] K. S. Reddy, “Thermal Modeling of PCM-based Solar Integrated Collector Storage Water Heating System”, *ASME Solar Energy Engineering*, vol. 129, pp. 458-464, 2007.

[8] C. Bellecci and M. Conti, “Transient Behaviour Analysis of a Latent Heat Thermal Storage Module”. *Int. J. Heat and Mass Transfer*, vol. 36, pp. 3851-3857, 1993.

[9] H. Ait Adine and H. El Qarnia, “Numerical Analysis of the Thermal Behaviour of a Shell-and-tube Heat Storage Unit Using Phase Change Materials”, *Applied Mathematical Modelling*, vol. 3, pp. 2132–2144, 2009.

[10] Y. B. Tao and Y. L. He, “Numerical Study on Thermal Energy Storage Performance of Phase Change Material Under non Steady State Inlet Boundary”. *Applied Energy*, vol. 88, pp. 4172–4179, 2011.